JACS
JOURNAL OF THE AMERICAN CHEMICAL SOCIETY
COMMUNICATION
pubs.acs.org/JACS

Low-*k* Periodic Mesoporous Organosilica with Air Walls: POSS-PMO

Makoto Seino,[†] Wendong Wang,[‡] Jennifer E. Lofgreen,[‡] Daniel P. Puzzo,[‡] Takao Manabe,[†] and Geoffrey A. Ozin*[,‡]

[†]Kaneka Corporation, 5-1-1, Torikai-nishi, Settsu, Osaka, Japan 566-0072

[‡]Lash Miller Chemical Laboratories, Department of Chemistry, University of Toronto, 80 Saint George Street, Toronto, Ontario, Canada M5S 3H6

S Supporting Information

ABSTRACT: Periodic mesoporous organosilica (PMO) with polyhedral oligomeric silsesquioxane (POSS) air pockets integrated into the pore walls has been prepared by a template-directed, evaporation-induced self-assembly spin-coating procedure to create a hybrid POSS-PMO thin film. A 10-fold increase in the porosity of the POSS-PMO film compared to a reference POSS film is achieved by incorporating ~1.5 nm pores. The increased porosity results in a decrease in the dielectric constant, *k*, which goes from 2.03 in a reference POSS film to 1.73 in the POSS-PMO film.

Periodic mesoporous organosilica (PMO) is a unique class of hybrid materials in which bridged organic groups are integrated into the silica pore walls.[1−3] PMOs have shown promise in diverse applications such as interconnect dielectrics for enabling smaller, faster, more powerful computer chips; an enhanced performance stationary phase for high resolution chromatography; targeted efficacious drug delivery vehicles; and molecular size selective catalytic sites.[4−9]

In the context of interconnect dielectrics, silicon dioxide served the microelectronics industry as a traditional dielectric material to insulate interconnect wiring.[10,11] However, with the down-scaling of device dimensions, the distance between adjacent wiring shrinks, thereby increasing resistance−capacitance (RC) delay and crosstalk between the adjacent wirings and consequently reducing the overall performance of the devices.[10−12] Circumventing these parasitic effects has necessitated a search for lower dielectric constant (low-*k*) materials other than silica.[9−11] The current low-*k* materials used in volume manufacturing are porous organics-added silica.[10,11] The incorporation of both organics and porosity lower the bulk *k* value of the materials.[11] In a similar fashion, the organics and porosity in PMOs make them ideal candidates for low-*k* materials.[13−16]

In this paper we go one step further by filling the pore walls of a PMO film with additional air pockets by making the organic group from a polyhedral oligomeric silsesquioxane (POSS), which has a nanosized cage structure with a ~0.3 nm pore as intramolecular space,[17,18] and describe herein the first example of a POSS-PMO thin film together with information on its structural, optical, and dielectric properties.

A POSS precursor, octa(triethoxysilylethyl)POSS (POSS-$[C_2H_4Si(OEt)_3]_8$) was synthesized by hydrosilylation of octavinyl POSS with triethoxysilane.[19,20] NMR spectra of POSS$[C_2H_4Si(OEt)_3]_8$ did not show signals of methylene and methyl groups

Scheme 1. Preparation of POSS-PMO Thin Film Using an EISA Spin-Coating Procedure

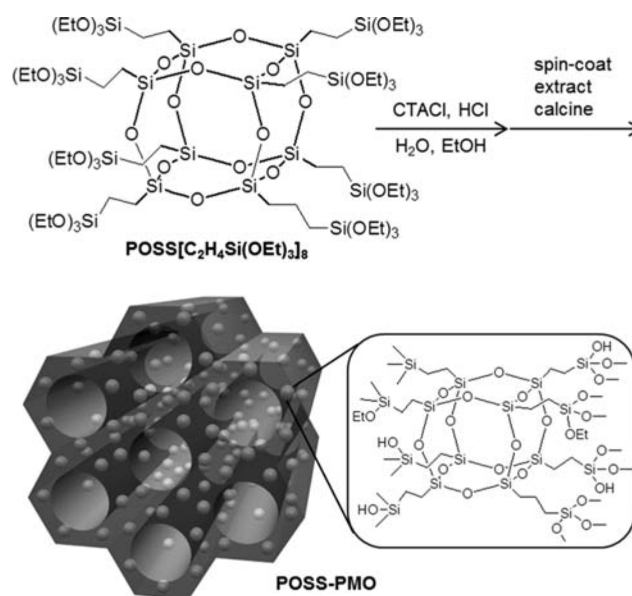

of an α-addition, indicating the hydrosilylation proceeds selectively via β-addition. The POSS-PMO thin film was prepared by an evaporation-induced self-assembly (EISA) spin-coating procedure (Scheme 1).[14] The POSS$[C_2H_4Si(OEt)_3]_8$ was mixed with a surfactant, cetyltrimethylammonium chloride (CTACl), hydrochloric acid aqueous solution, and ethanol at a predetermined, optimized ratio, and the mixture was stirred at room temperature for 30 min to form a transparent sol solution. The solution was coated on a silicon wafer by spin-coating at 3000 rpm for 20 s. The resulting film was dried in air at room temperature overnight and then was heated at 150 °C for 5 days under flowing nitrogen to increase the degree of condensation of the hydrolyzed POSS$[C_2H_4Si(OEt)_3]_8$. The CTACl template was extracted by washing the film with a solution of ethanol and hydrochloric acid. After the extraction, the film was further calcined at 300 °C under flowing nitrogen for 6 h.

Figure 1 shows X-ray diffraction (XRD) patterns of the as-spin-coated, extracted, and calcined films. The (100) diffraction peaks

Received: August 24, 2011
Published: October 26, 2011

ACS Publications © 2011 American Chemical Society

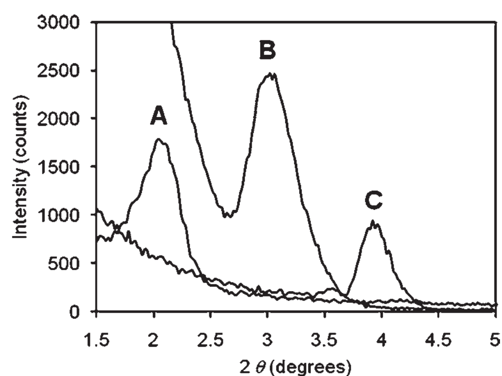

Figure 1. XRD patterns of POSS-PMO as (A) spin-coated film, (B) extracted film, and (C) calcined film.

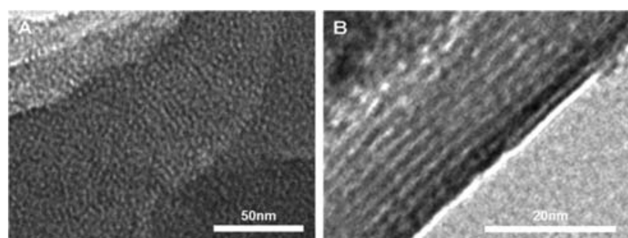

Figure 2. TEM images of the calcined POSS-PMO film: (A) showing the mesoporous structure and (B) showing the channel structure.

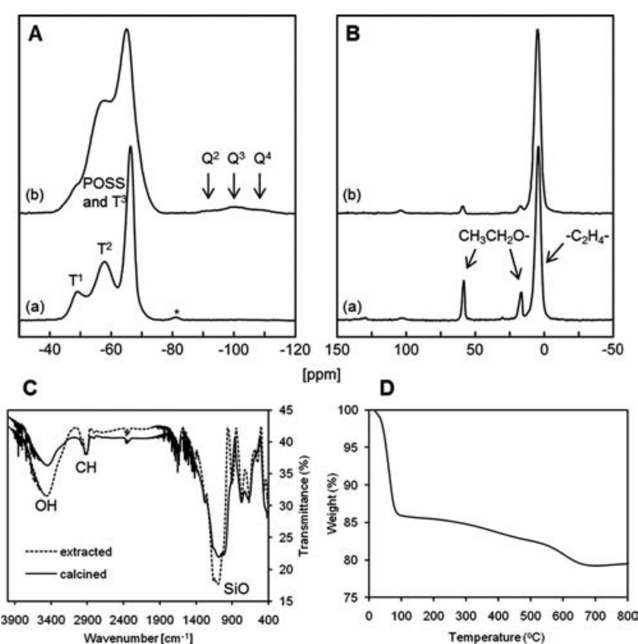

Figure 3. ^{29}Si (A) and ^{13}C (B) CP-MAS NMR spectra of the extracted (a) and calcined (b) POSS-PMO. (C) FTIR spectra of the extracted and calcined POSS-PMO films. (D) TGA profile of the extracted POSS-PMO film.

of these film samples are consistent with the presence of an ordered mesoporous structure. The increase in the intensity of the peak after the template extraction is due to an increase in electron contrast between the pores and channel walls.[14,15] The peaks of the extracted and calcined films are shifted to a higher angle, indicating the mesoporous structure contracts and the *d*-spacing decreases by further polycondensation of the hydrolyzed $POSS[C_2H_4Si(OEt)_3]_8$ during the heating process. There is a noticeable decrease in the XRD peak intensity of the calcined film, which most likely originates from some disordering of the mesoporous structure by cross-linked polycondensation of the multifunctional hydrolyzed $POSS[C_2H_4Si(OEt)_3]_8$.

Figure 2 shows transmission electron microscopy (TEM) images of fragments scratched from the POSS-PMO film calcined at 300 °C. They reveal the presence of channels with a pore diameter of ~1.5 nm, which is notably smaller than that of other PMO materials templated with CTACl.[14,15] This is consistent with the flexibility of the $POSS[C_2H_4Si(OEt)_3]_8$ precursor and the resulting contraction of the mesoporous structure upon polycondensation, template removal, and thermal treatment.

Figure 3A and B show the ^{29}Si and ^{13}C cross-polarization magic angle spinning (CP-MAS) NMR spectra of the fragments scratched from the extracted and calcined POSS-PMO thin film. The ^{29}Si CP-MAS NMR spectrum of the extracted POSS-PMO shows characteristic T_n signals ascribed to $CSi(OSi)_3$ (T_3), $CSi(OSi)_2OR$ (T_2), and $CSi(OSi)(OR)_2$ (T_1), where R is H or Et. The sharp and intense T_3 peak reveals that the cubic cage structure is retained during all stages of synthesis, template removal, and thermal post-treatment. Compared with the spectrum of the extracted POSS-PMO, the calcined one is broadened. Furthermore, small Q_n signals originating from $Si(OSi)_4$ (Q_4), $Si(OSi)_3OR$ (Q_3), and $Si(OSi)_2(OR)_2$ (Q_2) are observed, indicating that Si−C bond cleavage occurs during calcination, but only to a small degree. The ^{13}C CP-MAS spectra of both the extracted and calcined POSS-PMO show carbons of residual ethoxy groups as well as the ethylene linkage formed by hydrosilylation. The peaks ascribed to ethoxy groups in the spectrum of the calcined POSS-PMO are smaller than those of the extracted one, revealing further polycondensation of ethoxy groups during calcination. Figure 3C shows a comparison of the IR spectra between the extracted and calcined POSS-PMO films. The absorption area and hence the population of silanol groups are also decreased after calcination.

Figure 3D shows a thermogravimetric analysis (TGA) profile of the fragments of the template-extracted POSS-PMO thin film recorded under flowing nitrogen. About 14% mass loss attributed to physisorbed water is observed between 20 and 100 °C. The mass decreases by 1.13% from 100 to 300 °C, which is most likely due to a small loss of ethanol and water by the condensation of residual silanol and ethoxy groups as described above. This small loss of mass indicates that thermal decomposition of the POSS-PMO composite structure does not occur in the thermal post-treatment process. The mass continues to decrease gradually to a plateau at 79% of the original mass at ca. 700 °C. This decrease is ascribed to decomposition of some of the ethylene linkages of the POSS moiety and the loss of water and ethanol from the further condensation of residual silanol and ethoxy groups.

Selected physical properties of the calcined POSS-PMO film and a reference POSS film prepared without CTACl are estimated by ellipsometric porosimetry (EP) and surface acoustic wave spectroscopy (SAWS).[15,16] These results are summarized in Table 1. The porosity is calculated using the Clausius−Mossotti equation by comparing the difference between the refractive indices of the empty pores and the completely filled pores.[21] The value is 39.0% in contrast to 4.4% of the reference POSS film. The pore size, 1.56 nm (radius, 0.78 nm), is deduced

Table 1. POSS-PMO Thin Film Properties

sample	Porosity (%)[a]	Pore radius (nm)[a,b]	$d(100)$ (nm)[a]	Wall thickness (nm)[c]	E [EP] (GPa)[a]	E [SAWS] (GPa)[d]	k[e]	RI[a]
POSS-PMO film	39.0 ± 2.3	0.78 ± 0.04	2.33 ± 0.09	2.54 ± 0.1	2.66 ± 0.39	3.30 ± 0.14	1.73 ± 0.05	1.27 ± 0.01
POSS film	4.40 ± 0.5	–	–	–	–	29.6 ± 3.18	2.03 ± 0.07	1.44 ± 0.01

[a] The porosity, pore radius, $d(100)$, E[EP], and RI are obtained from four samples. [b] The pore radius is obtained from the adsorption branch of the isotherm with a contact angle of 57° (experimentally measured). [c] The wall thickness is calculated using $2d(100)/(3)^{1/2} - 2r_{pore}$. [d] The E[SAWS] are obtained from four measurements on a sample. [e] The k is obtained from measurements on four pads on a sample.

from the adsorption branch of the isotherm,[22] taking into account the effect of a contact angle, 57° in the Kelvin equation, which was determined macroscopically by measuring the angle between the solid−liquid interface and the liquid−air interface of a water droplet on the POSS-PMO film. Although the use of the concept of a contact angle becomes debatable when one considers pores of only a few nanometers,[23] we find that the pore diameter value obtained from EP (1.56 nm) and the value obtained from TEM images (∼1.5 nm) closely coincide. The Young's moduli obtained by EP and SAWS corresponded to the out-of-plane and in-plane Young's moduli.[15] In particular SAWS has been used for studying the Young's modulus of low-k thin films in the microelectronic industry.[24−26] It has been pointed out that the Young's modulus from SAWS higher than 4 GPa is sufficient for a low-k thin film to survive chemical mechanical polishing.[24] A value of 2.66 GPa obtained from EP is calculated by measuring the change in the thickness of the film during desorption and then using the Young−Laplace and Kelvin equations.[27] The value is comparable with those of PMOs having simple bridged organic groups.[15,16] A value of 3.30 GPa obtained from SAWS is close to that from EP, which is an unexpected result on the grounds that the Young's modulus from SAWS should have been higher than that from EP because the acoustic waves in SAWS propagate parallel to the surface along which the mesoporous channels are aligned.[15] Moreover, the value is smaller than those measured for common PMOs.[15,16] The most likely origin of this difference is the less ordered mesoporous structure of POSS-PMO. The capacitance is measured using the parallel plate method at 1 MHz, and the dielectric constant k is calculated with the equation $k = cd/A\epsilon_0$, where c is the observed capacitance, d is the film thickness which is measured by EP, A is the electrode pads area on the film, and ϵ_0 is the free permittivity. The k value for the POSS-PMO film is 1.73, which is significantly smaller than 2.03 of the reference POSS film, indicating the added porosity of the POSS-PMO film reduces the k value. The refractive index (RI) at 633 nm is also decreased with introduced porosity, going from 1.44 in the reference POSS film to 1.27 in the POSS-PMO film.

In summary, we have prepared the first example of a POSS-PMO thin film using an EISA spin-coating procedure. Although the POSS-PMO thin film shrinks during the template removal and thermal post-treatment process, the POSS cubic cage structure within the pore walls is retained and the mesoporous structure with an ∼1.5 nm pore size is maintained. About 40% porosity can be introduced into the POSS-PMO film, providing a reduced k value and lower RI of 1.73 and 1.27 respectively although the Young's modulus of 3.30 GPa from SAWS is slightly smaller than the stiffness limit of 4 GPa required for chemical mechanical polishing. We believe this favorable combination of the air holes and organic content of the POSS moiety together with the mesoporous structure of the PMO with subjection to continued refinement of its mechanical properties makes this hybrid POSS-PMO thin film an excellent potential candidate for low-k interlayer dielectric materials for the microelectronic industry.

ASSOCIATED CONTENT

Supporting Information. Experimental details of POSS precursor synthesis, POSS-PMO thin film preparation, instrumentation, and characterization. This material is available free of charge via the Internet at http://pubs.acs.org.

AUTHOR INFORMATION

Corresponding Author
gozin@chem.utoronto.ca

ACKNOWLEDGMENT

G.A.O. is the Government of Canada Research Chair in Materials Chemistry and Nanochemistry. We thank the Natural Sciences and Engineering Research Council (NSERC) of Canada and Kaneka Corporation of Japan for strong and sustained financial support of this work. S. Petrov is thanked for XRD measurements, D. Grozea for capacitance measurements, I. Moudrakovski for solid state NMR, and C. Andrei for TEM imaging.

REFERENCES

(1) Inagaki, S.; Guan, S.; Fukushima, Y.; Ohsuna, T.; Terasaki, O. *J. Am. Chem. Soc.* **1999**, *121*, 9611.
(2) Melde, B. J.; Holland, B. T.; Blanford, C. F.; Stein, A. *Chem. Mater.* **1999**, *11*, 3302.
(3) Asefa, T.; MacLachlan, M. J.; Coombs, N.; Ozin, G. A. *Nature* **1999**, *402*, 867.
(4) Hoffmann, F.; Cornelius, M.; Morell, J.; Froba, M. *Angew. Chem., Int. Ed.* **2006**, *45*, 3216.
(5) Fujita, S.; Inagaki, S. *Chem. Mater.* **2008**, *20*, 891.
(6) Hatton, B.; Landskron, K.; Whitnall, W.; Perovic, D.; Ozin, G. A. *Acc. Chem. Res.* **2005**, *38*, 305.
(7) Mizoshita, N.; Tani, T.; Inagaki, S. *Chem. Soc. Rev.* **2011**, *40*, 789.
(8) Wang, W.; Lofgreen, J. E.; Ozin, G. A. *Small* **2010**, *6*, 2634.
(9) Hatton, B. D.; Landskron, K.; Hunks, W. J.; Bennett, M. R.; Shukaris, D.; Perovic, D. D.; Ozin, G. A. *Mater. Today* **2006**, *9*, 22.
(10) Volksen, W.; Miller, R. D.; Dubois, G. *Chem. Rev.* **2010**, *110*, 56.
(11) Maex, K.; Baklanov, M. R.; Shamiryan, D.; Iacopi, F.; Brongersma, S. H.; Yanovitskaya, Z. S. *J. Appl. Phys.* **2003**, *93*, 8793.
(12) Miller, R. D. *Science* **1999**, *286*, 421.
(13) Lu, Y.; Fan, H.; Doke, N.; Loy, D. A.; Assink, R. A.; LaVan, D. A.; Brinker, C. J. *J. Am. Chem. Soc.* **2000**, *122*, 5258.
(14) Hatton, B. D.; Landskron, K.; Whitnall, W.; Perovic, D. D.; Ozin, G. A. *Adv. Funct. Mater.* **2005**, *15*, 823.
(15) Wang, W.; Grozea, D.; Kim, A.; Perovic, D. D.; Ozin, G. A. *Adv. Mater.* **2010**, *22*, 99.
(16) Wang, W.; Grozea, D.; Kohli, S.; Perovic, D. D.; Ozin, G. A. *ACS Nano* **2011**, *5*, 1267.

(17) Zhang, C.; Babonneau, F.; Bonhomme, C.; Laine, R. M.; Soles, C. L.; Hristov, H. A.; Yee, A. F. *J. Am. Chem. Soc.* **1998**, *120*, 8380.
(18) Cordes, D. B.; Lickiss, P. D.; Rataboul, F. *Chem. Rev.* **2010**, *110*, 2081.
(19) Su, R. Q.; Müller, T. E.; Procházka, J.; Lercher, J. A. *Adv. Mater.* **2002**, *14*, 1369.
(20) Zhang, L.; Abbenhuis, H. C. L.; Yang, Q.; Wang, Y.; Magusin, P. C. M. M.; Mezari, B.; van Santen, R. A.; Li., C. *Angew. Chem.* **2007**, *119*, 5091.
(21) Kobler, J.; Bein, T. *ACS Nano* **2008**, *2*, 2324.
(22) Kuemmel, M.; Grosso, D.; Boissière, C.; Smarsly, B.; Brezesinski, T.; Albouy, P. A.; Amenitsch, H.; Sanchez, C. *Angew. Chem., Int. Ed.* **2005**, *44*, 4589.
(23) Gregg, S. J.; Sing, K. S. W. *Adsorption, Surface Area, and Porosity*; Academic Press: London, 1982.
(24) Dubois, G.; Volksen, W.; Magbitang, T.; Miller, R. D.; Gage, D. M.; Dauskardt, R. H. *Adv. Mater.* **2007**, *19*, 3989.
(25) Dubois, G.; Volksen, W.; Magbitang, T.; Sherwood, M. H.; Miller, R. D.; Gage, D. M.; Dauskardt, R. H. *J. Sol-Gel Sci. Technol.* **2008**, *48*, 187.
(26) Oliver, M. S.; Dubois, G.; Sherwood, M.; Gage, D. M.; Dauskardt, R. H. *Adv. Funct. Mater.* **2010**, *20*, 2884.
(27) Mogilnikov, K. P.; Baklanov, M. R. *Electrochem. Solid-State Lett.* **2002**, *5*, F29.